The Rab GTPase RabG3b Positively Regulates Autophagy and Immunity-Associated Hypersensitive Cell Death in Arabidopsis[1][W]

Soon Il Kwon[2], Hong Joo Cho[2], Sung Ryul Kim, and Ohkmae K. Park*

School of Life Sciences and Biotechnology, Korea University, Seoul 136–701, Korea

A central component of the plant defense response to pathogens is the hypersensitive response (HR), a form of programmed cell death (PCD). Rapid and localized induction of HR PCD ensures that pathogen invasion is prevented. Autophagy has been implicated in the regulation of HR cell death, but the functional relationship between autophagy and HR PCD and the regulation of these processes during the plant immune response remain controversial. Here, we show that a small GTP-binding protein, RabG3b, plays a positive role in autophagy and promotes HR cell death in response to avirulent bacterial pathogens in Arabidopsis (*Arabidopsis thaliana*). Transgenic plants overexpressing a constitutively active *RabG3b* (RabG3bCA) displayed accelerated, unrestricted HR PCD within 1 d of infection, in contrast to the autophagy-defective *atg5-1* mutant, which gradually developed chlorotic cell death through uninfected sites over several days. Microscopic analyses showed the accumulation of autophagic structures during HR cell death in RabG3bCA cells. Our results suggest that RabG3b contributes to HR cell death via the activation of autophagy, which plays a positive role in plant immunity-triggered HR PCD.

In response to the constant attack by microbial pathogens, plants have developed defense mechanisms to protect themselves against harmful diseases caused by various pathogens. Plants primarily rely on two layers of innate immunity to cope with microbial pathogens (Jones and Dangl, 2006). The first layer of plant immunity, which is triggered by pathogen-associated molecular patterns (PAMPs) such as bacterial flagellin, lipopolysaccharides, and fungal chitin, is designated PAMP-triggered immunity (PTI; Boller and He, 2009). Because pathogens have evolved to overcome PTI, plants have developed a second layer of immunity, referred to as effector-triggered immunity (ETI; Dodds and Rathjen, 2010). ETI depends on specific interactions between plant Resistance proteins and pathogen effectors and is often associated with a form of programmed cell death (PCD) termed the hypersensitive response (HR), which inhibits pathogen growth (Coll et al., 2011).

Plants use PCD to regulate developmental and defense responses. In addition to pathogen attack, many abiotic stress factors such as heat and ozone exposure elicit PCD in plants (Hayward and Dinesh-Kumar, 2011). PCD also occurs during various developmental processes, including endosperm development, tracheary element (TE) differentiation, female gametophyte differentiation, leaf abscission, and senescence (Kuriyama and Fukuda, 2002; Gunawardena, 2008). Recently, plant PCD has been classified into two types, "autolytic" PCD and "nonautolytic" PCD, on the basis of the presence or absence of rapid cytoplasm clearance after tonoplast rupture, respectively (van Doorn et al., 2011). Autolytic PCD, which mainly occurs during plant development, falls under "autophagic" PCD in animals because it is associated with the accumulation of autophagy-related structures in the cytoplasm. Some forms of HR PCD classified as nonautolytic PCD in plants are accompanied by increased vacuolization, indicating the progress of autophagy, and therefore can be placed under autophagic PCD (Hara-Nishimura et al., 2005; Hatsugai et al., 2009).

Autophagy is an intracellular process in which double membrane-bound autophagosomes enclose cytoplasmic components and damaged or toxic materials and target them to the vacuole or lysosome for degradation (Chung, 2011). In plants, autophagy plays important roles in the responses to nutrient starvation, senescence, and abiotic and biotic stresses (Liu et al., 2005; Xiong et al., 2005, 2007; Bassham, 2007; Hofius et al., 2009). Accumulating evidence indicates that autophagy regulates immune responses in both animals and plants. Autophagy is essential for the direct elimination of pathogens in mammalian systems (Levine et al., 2011). Invading bacteria and viruses are targeted to autophagosomes and then delivered to the lysosome for degradation in a process

[1] This work was supported by the Next-Generation BioGreen 21 Programs through the Rural Development Administration (Plant Molecular Breeding Center, grant no. PJ008103032013; Systems and Synthetic Agrobiotech Center, grant no. PJ009580 to O.K.P.) and the Basic Science Research Program through the National Research Foundation (grant no. 2012–0007700 to S.I.K.).

[2] These authors contributed equally to the article.

* Corresponding author; e-mail omkim@korea.ac.kr.

The author responsible for distribution of materials integral to the findings presented in this article in accordance with the policy described in the Instructions for Authors (www.plantphysiol.org) is: Ohkmae K. Park (omkim@korea.ac.kr).

[W] The online version of this article contains Web-only data.

www.plantphysiol.org/cgi/doi/10.1104/pp.112.208108

called xenophagy (Levine, 2005). In addition to its function in directly killing pathogens, xenophagic degradation can provide microbial antigens for major histocompatibility complex class II presentation to the innate and adaptive immune systems (Levine, 2005; Schmid and Münz, 2007). Furthermore, the human surface receptor CD46 was shown to directly induce autophagy through physical interaction with the autophagic machinery (Joubert et al., 2009). The role of autophagy in plant basal immunity to virulent pathogens has been determined (Patel and Dinesh-Kumar, 2008; Hofius et al., 2009; Lai et al., 2011; Lenz et al., 2011). Arabidopsis (*Arabidopsis thaliana*) plants defective in *AUTOPHAGY-RELATED* (*ATG*) genes exhibited enhanced susceptibility to the necrotrophic fungal pathogens *Botrytis cinerea* and *Alternaria brassicicola*, suggesting that the massive breakdown of cytoplasmic materials provides nutrients for the growth of necrotrophic pathogens or that fungal toxin-induced necrotic cell death is enhanced in *atg* mutants (Lai et al., 2011; Lenz et al., 2011). However, studies on the responses to the biotrophic pathogen *Pseudomonas syringae* pv *tomato* DC3000 (*Pst* DC3000) have yielded contradictory results. Whereas earlier studies reported that bacterial numbers significantly increased in *ATG6*-antisense (*AS*) and *atg* mutant plants (Patel and Dinesh-Kumar, 2008; Hofius et al., 2009), a recent study indicated that *atg* mutants exhibit increased resistance to *Pst* DC3000 (Lenz et al., 2011). Although these discrepancies remain to be resolved, salicylic acid (SA) levels and SA-dependent gene expression were both elevated in *atg* mutants, suggesting that autophagy may negatively regulate SA-associated plant immunity (Yoshimoto et al., 2009; Lenz et al., 2011). These findings indicate that the role of autophagy in plant immunity depends on the lifestyle of the invading pathogens (Lenz et al., 2011).

Autophagy plays an important role in the regulation of HR PCD in plant innate immunity (Hayward and Dinesh-Kumar, 2011). Tobacco (*Nicotiana tabacum*) plants silenced for *ATG6/Beclin1* and other *ATG* genes such as *phosphatidylinositol 3-kinase (PI3K)/vacuolar protein sorting34 (VPS34)*, *ATG3*, and *ATG7* underwent unrestricted HR PCD upon pathogen infection (Liu et al., 2005). *ATG6-AS* and *atg5* mutant Arabidopsis plants also displayed unlimited HR PCD upon infection with the avirulent bacterium *Pst* DC3000 (*AvrRpm1*; Patel and Dinesh-Kumar, 2008; Yoshimoto et al., 2009). These studies suggest that autophagy is a "prosurvival" or "antideath" mechanism that negatively regulates HR PCD (Liu and Bassham, 2012). By contrast, a "prodeath" role has been suggested for autophagy in HR PCD regulation (Hofius et al., 2009). *Pst* DC3000 (*AvrRps4*)-induced and, to a lesser extent, *Pst* DC3000 (*AvrRpm1*)-induced HR PCD was suppressed in *atg* mutants, suggesting that autophagy plays a positive role and that autophagic cell death is involved in RPS4- and RPM1-mediated HR cell death.

We previously showed that the small GTP-binding protein RabG3b, isolated from secretome analysis in Arabidopsis (Oh et al., 2005), functions as a component of autophagy and positively regulates TE differentiation via the activation of autophagic cell death (Kwon et al., 2010a, 2010b). Overexpression of a constitutively active *RabG3b* (RabG3bCA) in plants significantly increased autophagy during PCD associated with TE differentiation, thereby enhancing TE formation and xylem development. Transgenic poplar (*Populus alba* × *Populus tremula* var *glandulosa*) overexpressing Arabidopsis RabG3bCA was further generated, and these exhibited significant stimulation of xylem development together with autophagic activation, suggesting that RabG3b is a positive regulator of autophagy and xylem development in *Populus* spp. as well as Arabidopsis (Kwon et al., 2011). We also reported that RabG3b is involved in cell death associated with the fungal pathogen *A. brassicicola* and infection with the fungal toxin fumonisin B1 (FB1) as well as leaf senescence (Kwon et al., 2009). Here, we extend our work to determine the role of RabG3b and autophagy in immunity-associated HR PCD. We found that RabG3bCA transgenic plants accumulated a large number of autophagic structures and displayed accelerated, expanded cell death against a number of PCD inducers, such as FB1 and the bacterial pathogens *Pst* DC3000 (*AvrRpm1*) and *Pst* DC3000 (*AvrRpt2*). Our results suggest that RabG3b plays a positive role in immunity-associated HR PCD via the activation of autophagic cell death.

RESULTS

RabG3b Positively Regulates Pathogen-Induced Hypersensitive Cell Death

Our previous studies showed that RabG3b positively regulates TE PCD through autophagic activation in Arabidopsis, suggesting a positive role of autophagy in developmental PCD (Kwon et al., 2010a). Here, we address whether RabG3b is additionally involved in pathogen-induced HR PCD and whether its role is autophagy related. In this study, we used an autophagy-defective mutant, *atg5-1*, and three different *RabG3b* transgenic plants overexpressing constitutively active *RabG3b* (RabG3bCA), dominant negative *RabG3b* (RabG3bDN), and an RNA interference construct of *RabG3b* (RabG3bRNAi), as described previously (Kwon et al., 2010a). In a previous report (Yoshimoto et al., 2009), unlimited cell death was observed upon challenge with *Pst* DC3000 (*AvrRpm1*) in 7- to 8-week-old "old" *atg5-1* plants grown under short-day conditions but not in 4- to 5-week-old "young" *atg5-1* plants, indicating that plant age is important for cell death development. Thus, we first examined cell-death phenotypes of old plants grown under short-day conditions (Fig. 1, A and B). Hypersensitive local cell death was readily induced within hours of inoculation and formed a clear necrotic lesion within 1 to 2 d in all tested plants; however, it expanded to the entire infected leaf in RabG3bCA plants within 2 d, whereas the other plants did not exhibit the accelerated, spreading cell-death phenotype (Fig. 1A). Consistently, the infected leaves

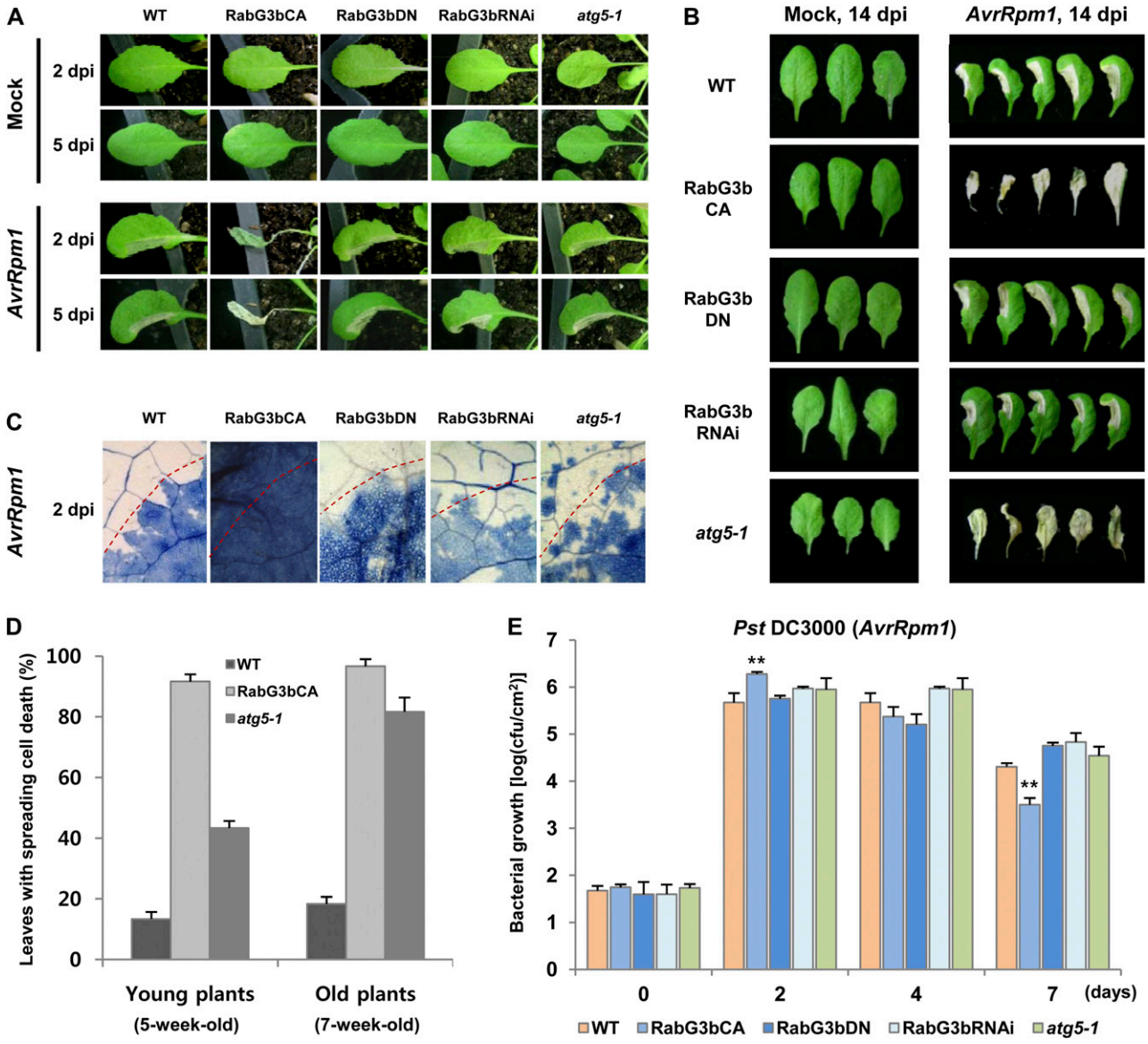

Figure 1. *Pst* DC3000 (*AvrRpm1*)-induced HR cell death is enhanced in RabG3bCA plants. A, Phenotypes of wild-type (WT), RabG3bCA, RabG3bDN, RabG3bRNAi, and *atg5-1* leaves inoculated with 10 mM $MgCl_2$ (Mock) or 10^8 cfu mL^{-1} *Pst* DC3000 (*AvrRpm1*) for 2 and 5 d. B, Phenotypes of wild-type, RabG3bCA, RabG3bDN, RabG3bRNAi, and *atg5-1* leaves inoculated with 10 mM $MgCl_2$ (Mock) or 10^8 cfu mL^{-1} *Pst* DC3000 (*AvrRpm1*) for 14 d. C, Cell death in leaves stained with trypan blue. Leaves inoculated with 10^8 cfu mL^{-1} *Pst* DC3000 (*AvrRpm1*) for 2 d as in B were used for staining. D, Quantitative analysis of spreading cell death in leaves of young (5-week-old) and old (7-week-old) wild-type, RabG3bCA, and *atg5-1* plants at 14 d post inoculation with *Pst* DC3000 (*AvrRpm1*). Results represent means ± SD from five independent experiments ($n = 30$). E, Bacterial growth in wild-type, RabG3bCA, RabG3bDN, RabG3bRNAi, and *atg5-1* plants inoculated with 10^5 cfu mL^{-1} *Pst* DC3000 (*AvrRpm1*). Results represent means ± SD ($n = 4$). Asterisks indicate significant differences from the respective wild type (Student's *t* test; $^{**}P < 0.01$). These experiments were performed five times with similar results. dpi, Days post inoculation.

of RabG3bCA plants were entirely stained with trypan blue, which specifically stains dead cells (Fig. 1C). As reported previously (Yoshimoto et al., 2009), *atg5-1* plants slowly spread chlorotic cell death following prolonged incubation with *Pst* DC3000 (*AvrRpm1*) over 14 d (Fig. 1B). Trypan blue staining showed that cell death gradually spread beyond the infection site in the *atg5-1* mutant, even without visible cell death symptoms at 2 d after pathogen treatment (Fig. 1C). Young plants were then challenged with *Pst* DC3000 (*AvrRpm1*), and RabG3bCA plants exhibited a similar accelerated, spreading HR cell-death phenotype (Supplemental Fig. S1). The occurrence rates of the spreading HR PCD in leaves were comparable in old and young RabG3bCA plants (97% versus 93%, respectively; Fig. 1D). On the other hand, *Pst* DC3000

(*AvrRpm1*)-infiltrated leaves of young *atg5-1* plants exhibited a progression of spreading chlorotic cell death, like those of old plants, but with a considerable reduction in the occurrence rates of spreading cell death (82% in old plants versus 43% in young plants). Similar results were obtained with another avirulent pathogen, *Pst* DC3000 (*AvrRpt2*; Supplemental Fig. S2). These findings suggest that two distinct types of cell death occur in plants challenged with avirulent bacterial pathogens: hypersensitive necrotic cell death and chlorotic cell death. Whereas the former, so-called HR PCD, rapidly occurred at the infection sites within hours and expanded in RabG3bCA plants, the latter gradually spread over days through uninfected sites, depending on plant age, and was associated with autophagy deficiency.

To further determine whether the spreading lesion induced by pathogen treatments in RabG3bCA plants was a consequence of uncontrolled cell death, we monitored the cell-death phenotype following treatment with the well-known PCD-eliciting mycotoxin FB1 (Supplemental Fig. S2). As observed with pathogen infection, FB1-treated RabG3bCA leaves displayed accelerated, spreading cell death, in contrast to other plants. RabG3bDN, RabG3bRNAi, and wild-type plants did not significantly differ in cell death symptom development in response to all the treatments tested (Fig. 1; Supplemental Fig. S2). Collectively, these results demonstrate that RabG3b is associated with cell death-promoting activity during hypersensitive PCD.

We then examined bacterial growth in plants inoculated with *Pst* DC3000 (*AvrRpm1*; Fig. 1E). Although *Pst* DC3000 (*AvrRpm1*) growth increased for 2 d after pathogen inoculation in RabG3bCA plants, bacterial growth gradually decreased thereafter, and bacterial numbers in RabG3bCA leaves were 6.2-fold lower than in wild-type leaves 7 d after inoculation (Fig. 1E). Thus, although RabG3bCA plants were not able to fully restrict bacterial growth during the early stage of infection, they readily restored the activity necessary to suppress bacterial growth, indicating that expanded cell death in RabG3bCA plants is not due to increased bacterial growth. Bacterial growth in the *atg5-1* mutant was not significantly different from that in wild-type, RabG3bDN, and RabG3bRNAi plants. Similar bacterial growth results were obtained with *Pst* DC3000 (*AvrRpt2*; Supplemental Fig. S3).

In a previous study, the electrolyte leakage test was used to assess the development of pathogen-induced HR cell death in *atg* mutants (Hofius et al., 2009). Here, we performed the electrolyte leakage assay and compared the extent of HR cell death in wild-type, RabG3bCA, and *atg5-1* leaves inoculated with *Pst* DC3000 (*AvrRpm1*) and *Pst* DC3000 (*AvrRpt2*; Fig. 2). Both *Pst* DC3000 (*AvrRpm1*) and *Pst* DC3000 (*AvrRpt2*) infection enhanced electrolyte leakage and, consequently, conductance in plants. Whereas this increase was considerably suppressed in *atg5-1* leaves infected with *Pst* DC3000 (*AvrRpm1*), more leakage was observed with *Pst* DC3000 (*AvrRpt2*). This is in agreement with the previous study by Hofius et al. (2009), suggesting that autophagy is involved in *AvrRpm1*-triggered cell death but is minimally involved in *AvrRpt2*-induced cell death. In contrast, RabG3bCA plants exhibited higher electrolyte leakage than the wild type upon infection with either *Pst* DC3000 (*AvrRpm1*) or *Pst* DC3000 (*AvrRpt2*). These data support a positive role for RabG3b in pathogen-induced hypersensitive cell death.

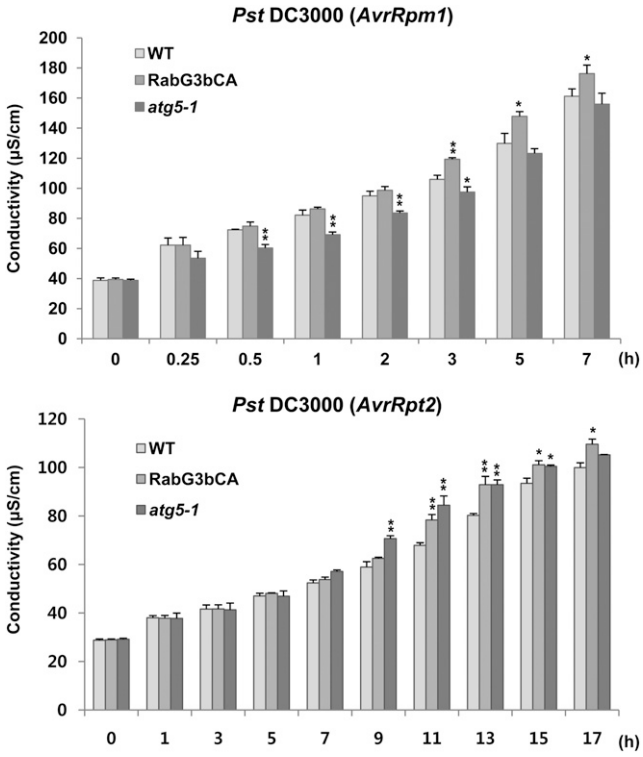

Figure 2. Ion leakage assays in wild-type (WT), RabG3bCA, and *atg5-1* plants inoculated with *Pst* DC3000 (*AvrRpm1*; top) and *Pst* DC3000 (*AvrRpt2*; bottom). Leaves of 5-week-old plants were infiltrated with *Pst* DC3000 (*AvrRpm1*) and *Pst* DC3000 (*AvrRpt2*) at 10^8 cfu mL^{-1}. Results represent means ± SD ($n = 10$). Asterisks indicate significant differences from the respective wild-type (Student's *t* test; $*P < 0.05$, $**P < 0.01$). These experiments were performed three times with similar results.

Basal Immunity Is Not Altered in RabG3bCA Plants

Accumulating evidence indicates that PTI and ETI use common signaling pathway components, although ETI elicits more prolonged and robust immune responses than PTI and is associated with HR PCD (Tsuda and Katagiri, 2010). PAMPs also induce cell death, but their effect is weak compared with that of ETI-triggered cell death. However, flagellin from *P. syringae* pv *tabaci* 6605 was shown to strongly induce cell death (Naito et al., 2008). This suggests that PTI and ETI may also share common signaling machinery leading to immunity-induced cell death. Therefore, we investigated whether the expanded cell death in RabG3bCA plants infected

with avirulent bacterial pathogens was due to any defects in basal immunity. PTI responses such as callose deposition and gene expression were examined in plants challenged with the PAMP flagellin (flg22; Lenz et al., 2011). The induction of callose deposition and the expression of PTI molecular marker genes *FRK1* and *PR1* were indistinguishable in wild-type, *atg5-1*, and RabG3bCA plants (Supplemental Fig. S4, A and B). These results indicate that basal immunity is not altered and is irrelevant to the uncontrolled cell death observed in RabG3bCA and *atg5-1* plants. Bacterial growth was then examined in plants inoculated with *Pst* DC3000 (Supplemental Fig. S4C). Bacterial growth decreased in the *atg5-1* mutant but rather increased in RabG3bCA plants. This suggests that autophagy plays a negative role in SA-associated plant immunity to bacterial infection, and this does not occur through altered PTI responses, as reported previously (Yoshimoto et al., 2009; Lenz et al., 2011).

RabG3b Activates Autophagy during Hypersensitive Cell Death

Given that RabG3b positively regulates TE PCD by activating autophagy (Kwon et al., 2010a, 2010b), we

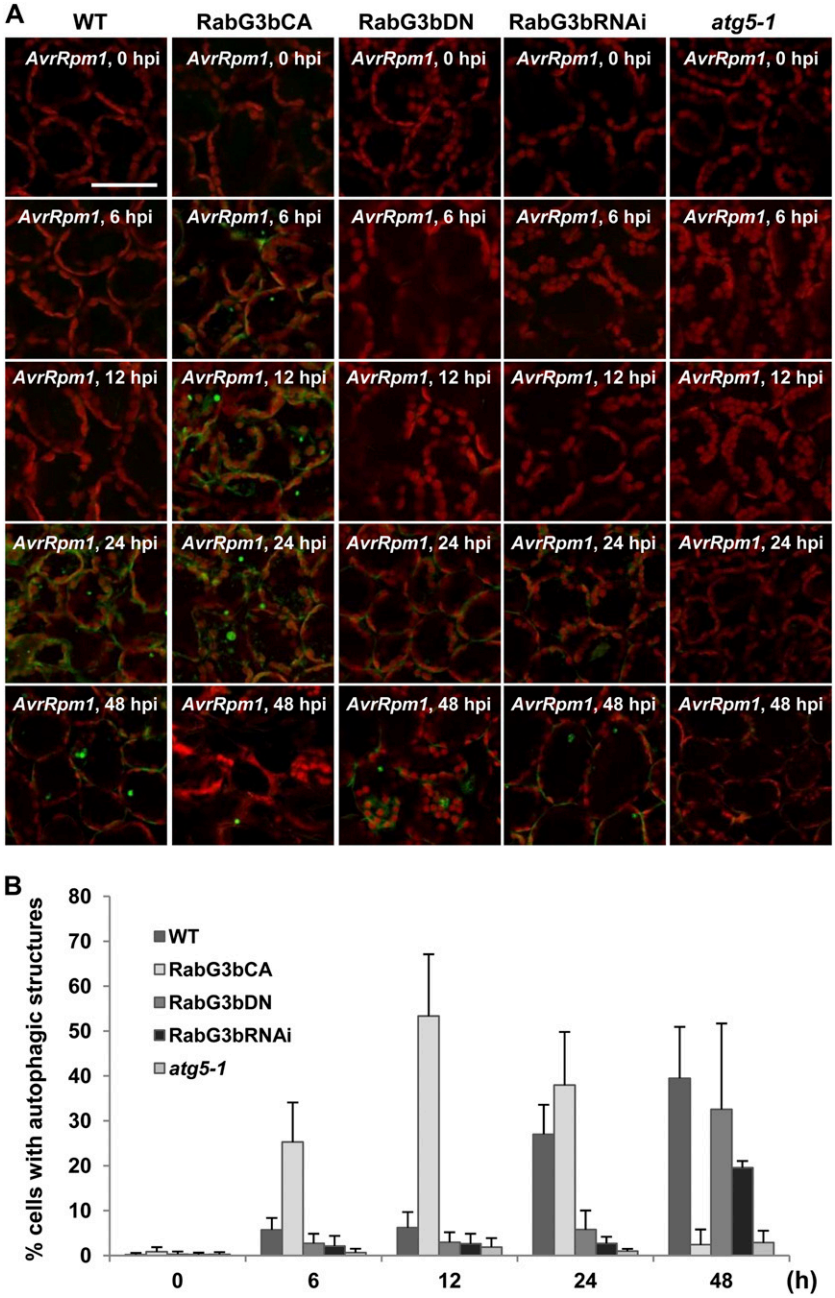

Figure 3. Autophagic structures accumulate in wild-type plants (WT) and more abundantly in RabG3bCA plants following *Pst* DC3000 (*AvrRpm1*) infection. A, LTG staining of mesophyll cells at the infected sites of wild-type, RabG3bCA, RabG3bDN, RabG3bRNAi, and *atg5-1* plants treated with 10^6 cfu mL^{-1} *Pst* DC3000 (*AvrRpm1*) for 0, 6, 12, 24, and 48 h. hpi, Hours post inoculation. Bar = 50 μm. B, Quantitative analysis of LTG-stained structures in A. Stained tissues were photographed, and cells with fluorescent spots were counted per 250-μm^2 area. Results represent means ± SD ($n = 6$). These experiments were performed three times with similar results.

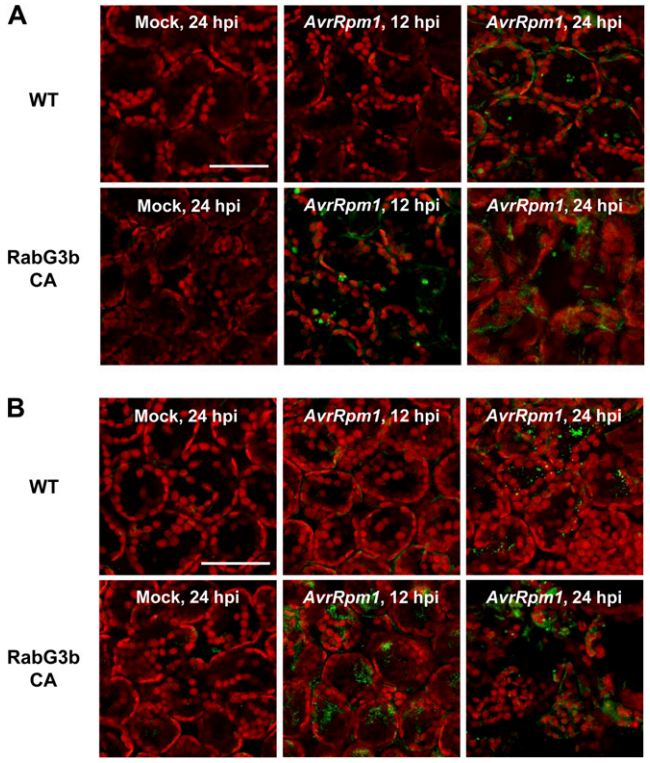

Figure 4. ATG8a-associated autophagosome structures accumulate in *Pst* DC3000 (*AvrRpm1*)-infected RabG3bCA plants. A, LTG staining of mesophyll cells from wild-type (WT) and RabG3bCA plants treated with 10 mM $MgCl_2$ (Mock) or 10^6 cfu mL^{-1} *Pst* DC3000 (*AvrRpm1*) for 12 and 24 h. B, Whole-mount immunofluorescence staining of mesophyll cells of the wild-type and RabG3bCA plants described in A with the anti-ATG8a antibody. hpi, Hours post inoculation. Bars = 50 μm.

investigated whether the expanded HR PCD in RabG3bCA plants was also associated with autophagic activation. Wild-type, RabG3bCA, RabG3bDN, RabG3bRNAi, and *atg5-1* plants were treated with *Pst* DC3000 (*AvrRpm1*), and autophagy was monitored over time in mesophyll cells of infected tissues by staining with LysoTracker Green (LTG), which stains acidic organelles including autophagosome and autolysosome structures (Fig. 3; Via et al., 1998; Liu et al., 2005; Hofius et al., 2009). In wild-type plants, *Pst* DC3000 (*AvrRpm1*) treatment induced the formation of LTG-stained autophagic structures 24 h after treatment. On the other hand, LTG-stained punctate structures were detected earlier in *Pst* DC3000 (*AvrRpm1*)-infected RabG3bCA plants at 6 h post infection and accumulated to higher levels than in treated wild-type plants. The disappearance of LTG-stained structures from RabG3bCA leaves at 48 h post infection resulted from severe cell death and complete collapse of subcellular organelles and structures. LTG-stained structures were also detected at the uninfected sites in both wild-type and RabG3bCA plants, although later than those at the infected sites (Supplemental Fig. S5). RabG3bDN and RabG3bRNAi plants also displayed LTG-stained structures at 24 and 48 h post infection, more slowly than the wild type (Fig. 3). By contrast, LTG-stained structures were rarely detected in *atg5-1* plants.

As LTG is a nonspecific acidotropic dye, autophagosome structures were specifically stained by whole-mount immunofluorescence using the anti-ATG8a antibody and compared with LTG-stained structures (Fig. 4). LTG-stained and ATG8a-associated autophagosome structures were identified in *Pst* DC3000 (*AvrRpm1*)-treated cells with similar timing and patterns, confirming that *Pst* DC3000 (*AvrRpm1*)-infected RabG3bCA leaves develop abundant autophagic structures earlier than the wild type. We further examined the induction of autophagy by western-blot analysis using the anti-ATG8a antibody. Formation of the ATG8-phosphatidylethanolamine (PE) conjugate was monitored as a marker for autophagic activation (Fig. 5). In addition to free ATG8 proteins, the faster migrating ATG8-PE adduct was detected at 8 h after *Pst* DC3000 (*AvrRpm1*) inoculation in wild-type plants, whereas the ATG8-PE band appeared earlier at 4 h post infection and was more abundant in *Pst* DC3000 (*AvrRpm1*)-infected RabG3bCA plants.

Prior studies showed that the induction of autophagy during HR PCD depends on the type of immune receptor, Toll/Interleukin-1 receptor (TIR)-nucleotide binding (NB)-Leu-rich repeat (LRR) or coiled-coil (CC)-NB-LRR, activated by different bacterial avirulent factors (Hofius et al., 2009). In contrast to *Pst* DC3000 (*AvrRpm1*), *Pst* DC3000 (*AvrRpt2*) infection induced only weak accumulation of LTG-stained structures in wild-type plants, suggesting that *AvrRpt2*-triggered HR cell death may be independent of autophagy (Hofius

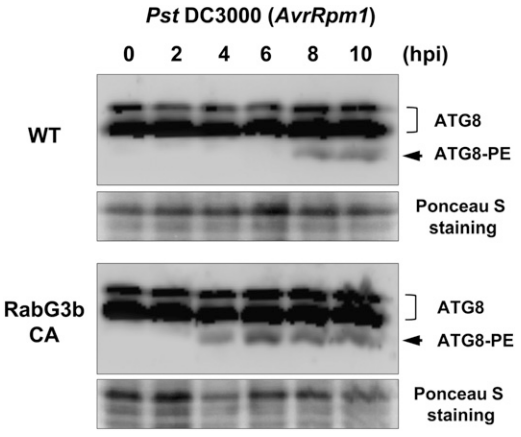

Figure 5. Western-blot analysis for detection of the ATG8-PE adduct in wild-type (WT) and RabG3bCA plants after *Pst* DC3000 (*AvrRpm1*) treatment. Total proteins were extracted from leaves treated with 1×10^6 cfu mL^{-1} *Pst* DC3000 (*AvrRpm1*) for the indicated times, separated by SDS gel electrophoresis in the presence of 6 M urea, and subjected to western-blot analysis with the anti-ATG8a antibody. The blots were stained with Ponceau S to assess protein loading. hpi, Hours post inoculation.

et al., 2009). Therefore, we checked for autophagic structures in wild-type and RabG3bCA plants challenged with *Pst* DC3000 (*AvrRpt2*; Supplemental Fig. S6A). Wild-type plants gradually accumulated LTG-stained structures during the course of *Pst* DC3000 (*AvrRpt2*) infection, although at a much lower level than in *Pst* DC3000 (*AvrRpm1*)-treated plants, as reported previously (Hofius et al., 2009). However, RabG3bCA plants developed a higher number of punctate structures in response to *Pst* DC3000 (*AvrRpt2*) than wild-type plants, suggesting that autophagy was at least partly involved in HR PCD induced by *Pst* DC3000 (*AvrRpt2*). Additional examination using transmission electron microscopy (TEM) revealed autophagosome structures in *Pst* DC3000 (*AvrRpt2*)-infected leaves (Supplemental Fig. S6B). Collectively, these results demonstrate that autophagy is activated in wild-type plants and that this activation is enhanced in RabG3bCA plants during *AvrRpm1*- and *AvrRpt2*-triggered hypersensitive PCD.

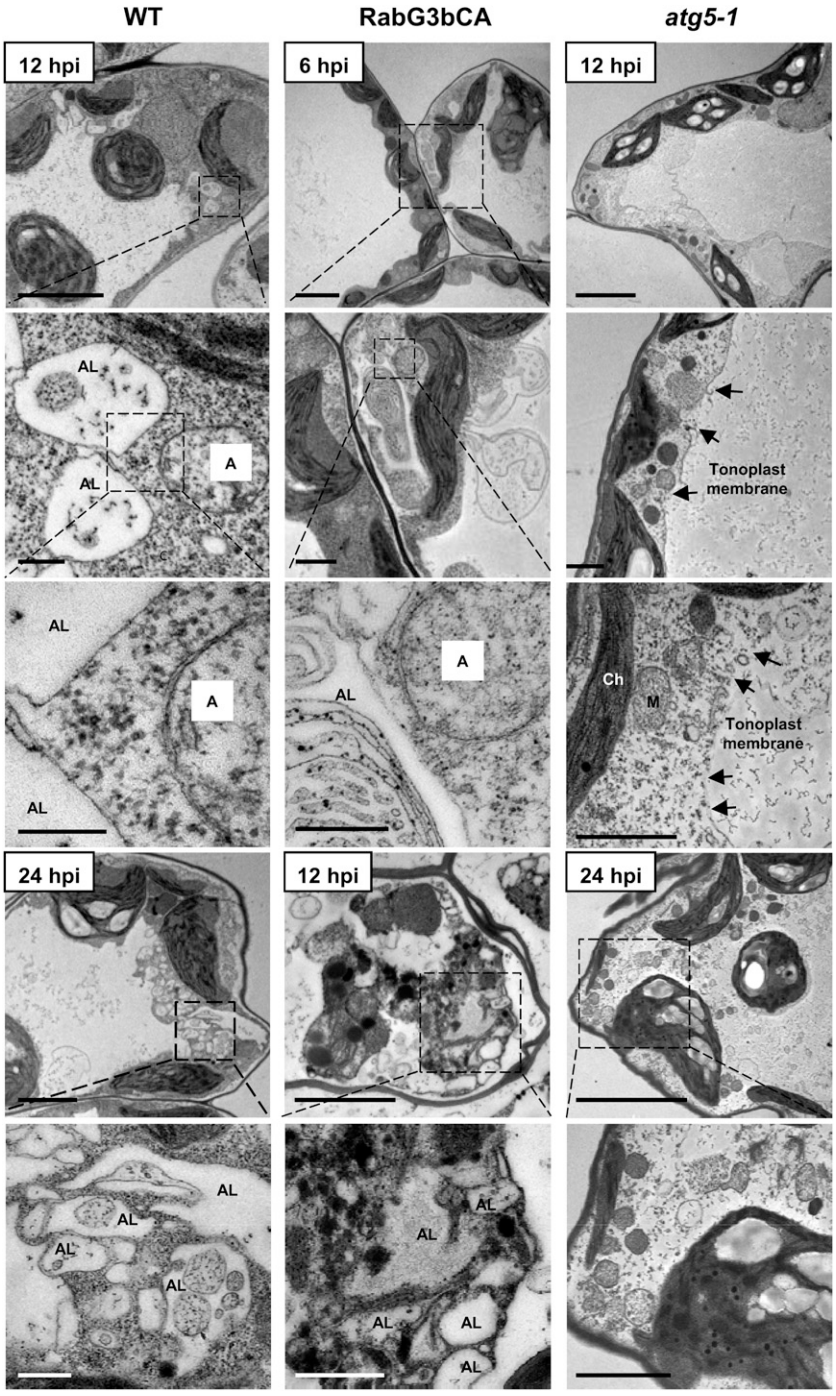

Figure 6. TEM images of autophagic structures in wild-type (WT), RabG3bCA, and *atg5-1* plants inoculated with *Pst* DC3000 (*AvrRpm1*). Plant leaves were treated with 10^6 cfu mL^{-1} *Pst* DC3000 (*AvrRpm1*) for the indicated times and subjected to TEM analysis. Enlarged images of the boxed areas are shown below. Images are representative of those obtained from three independent experiments. Arrows indicate rupture of the tonoplast membrane. A, Autophagosome; AL, autolysosome; Ch, chloroplast; hpi, hours post inoculation; M, mitochondria. Bars = 5 μm (top) and 200 nm (middle and bottom) for 12 hpi (wild type and *atg5-1*) and 6 hpi (RabG3bCA) and 5 μm (top) and 1 μm (bottom) for 24 hpi (wild type and *atg5-1*) and 12 hpi (RabG3bCA).

RabG3bCA Cells Accumulate Abundant Autophagic Structures during Pathogen-Induced Hypersensitive Cell Death

TEM analysis was performed to confirm the results from LTG staining, immunofluorescence, and immunoblotting and to examine the ultrastructure of cells during *Pst* DC3000 (*AvrRpm1*)-induced HR cell death (Fig. 6; Supplemental Fig. S7). Wild-type, RabG3bCA, and *atg5-1* cells showed no differences in subcellular morphology before pathogen treatment (Supplemental Fig. S7). However, *Pst* DC3000 (*AvrRpm1*) infection caused drastic changes in subcellular structures, including the degradation of cell contents (Fig. 6; Supplemental Fig. S7). During the initial stages (within 24 h) of infection, wild-type and RabG3bCA plants formed numerous autophagosome and autolysosome structures containing degrading organelles and cytoplasmic constituents and simultaneously accumulated damaged structures, including plastids, suggesting that autophagy contributes to the cell death process (Fig. 6). Over time, wild-type and RabG3bCA cells underwent progressive shrinking, and cellular components appeared as electron-dense materials, indicative of dying cells (Fig. 6; Supplemental Fig. S7). Similar patterns of autophagic structures and ultrastructural changes were observed in wild-type and RabG3bCA cells in response to *Pst* DC3000 (*AvrRpm1*) infection, although at an earlier time and with increased expansion in RabG3bCA cells than in the wild type. By contrast, *Pst* DC3000 (*AvrRpm1*)-inoculated *atg5-1* leaves showed no obvious autophagic features but underwent gradual degradation of cellular components (Fig. 6; Supplemental Fig. S7). Vacuolar membrane collapse was often observed, suggesting that the release of vacuolar hydrolytic enzymes into the cytosol may be the cause of cell death in the *atg5-1* mutant (Fig. 6).

The localization of RabG3b proteins to autophagic structures was analyzed by immunogold electron microscopy using antibodies against RabG3b and the autophagosome marker protein ATG8a in *Pst* DC3000 (*AvrRpm1*)-infected wild-type and RabG3bCA cells (Fig. 7). In mock-treated cells, RabG3b and ATG8a proteins were detected in the cytosol. Upon *Pst* DC3000 (*AvrRpm1*) infection, ATG8a protein levels were greatly elevated and mostly associated with autophagic structures, and RabG3b proteins were colocalized with ATG8a proteins in autophagic structures in both wild-type and RabG3bCA cells. This further demonstrates that RabG3b function is closely associated with autophagy during pathogen-induced HR cell death.

RabG3b-Associated Autophagy Is Partially ATG5 Dependent during Hypersensitive Cell Death

It was further assessed whether the HR cell death and autophagic activation in RabG3bCA plants was related to ATG5-mediated autophagy. We crossed RabG3bCA and *atg5-1* mutant plants and obtained homozygous crossing lines. We examined HR cell death phenotypes in RabG3bCA, *atg5-1*, and RabG3bCA *atg5-1* plants after *Pst* DC3000 (*AvrRpm1*) treatment (Fig. 8). Hypersensitive necrotic cell death was observed, but its progression was significantly slower and less expanded in *Pst* DC3000 (*AvrRpm1*)-infiltrated RabG3bCA *atg5-1* leaves compared with RabG3bCA plants, and it was often preceded by chlorotic cell death spreading beyond the infected site, as in *atg5-1* plants. Bacterial growth was then examined in plants inoculated with *Pst* DC3000 (*AvrRpm1*) or *Pst* DC3000 (*AvrRpt2*; Supplemental Fig. S8). Bacterial growth in RabG3bCA *atg5-1* plants was not significantly different from that in wild-type and *atg5-1* plants.

We then investigated the formation of autophagic structures in the infected leaves by LTG staining (Fig. 9). Whereas *Pst* DC3000 (*AvrRpm1*) induced the formation of LTG-stained autophagic structures in RabG3bCA

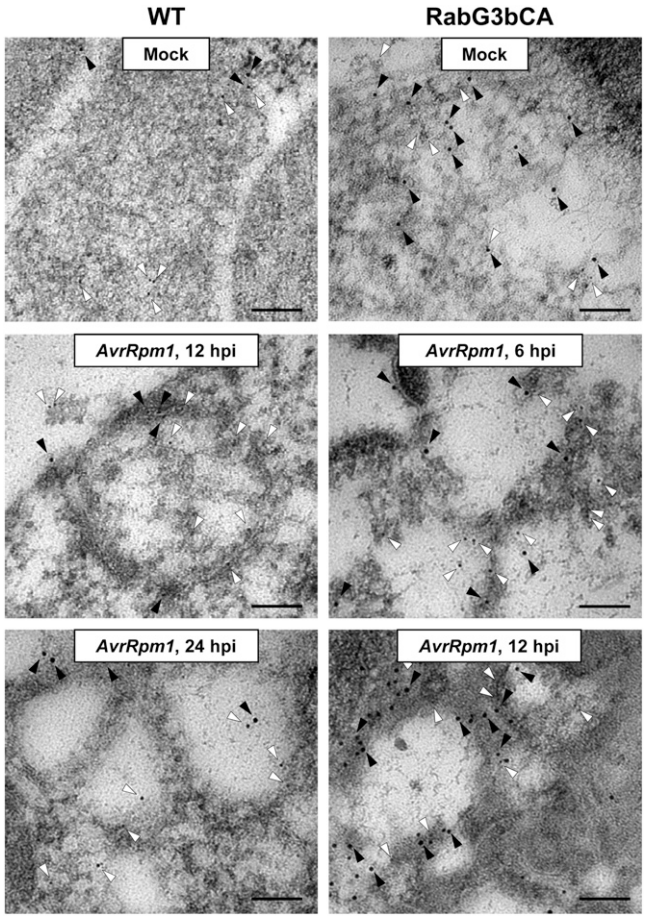

Figure 7. RabG3b colocalizes with ATG8a in autophagic structures. Plant leaves were treated with 10 mM $MgCl_2$ (Mock) or 10^6 cfu mL^{-1} *Pst* DC3000 (*AvrRpm1*) for the indicated times and subjected to immunogold labeling. Black and white arrowheads mark RabG3b (5-nm gold) and ATG8a (1-nm gold), respectively. hpi, Hours post inoculation WT, wild type. Bars = 100 nm.

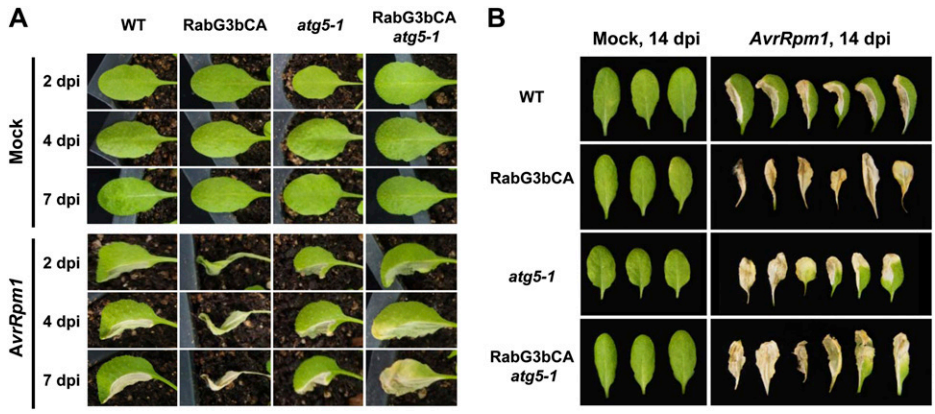

Figure 8. *Pst* DC3000 (*AvrRpm1*)-induced HR cell death in RaG3bCA *atg5-1*, RabG3bCA, and *atg5-1* plants. A, Phenotypes of wild-type (WT), RabG3bCA, *atg5-1*, and RabG3bCA *atg5-1* leaves inoculated with 10 mM $MgCl_2$ (Mock) or 10^8 cfu mL^{-1} *Pst* DC3000 (*AvrRpm1*) for 2, 4, and 7 d. B, Phenotypes of wild-type, RabG3bCA, *atg5-1*, and RabG3bCA *atg5-1* leaves inoculated with 10 mM $MgCl_2$ (Mock) or 10^8 cfu mL^{-1} *Pst* DC3000 (*AvrRpm1*) for 14 d. dpi, Days post inoculation.

plants at 6 h post infection and increased up to 24 h post infection, LTG-stained structures were detected later at 24 h post infection in RabG3bCA *atg5-1* leaves. Whole-mount immunofluorescence staining of *Pst* DC3000 (*AvrRpm1*)-infected RabG3bCA *atg5-1* leaves with the anti-ATG8a antibody verified that LTG-stained structures were ATG8a-associated autophagic structures (Supplemental Fig. S9). By contrast, no LTG- and ATG8a-stained structures were detected in *atg5-1* plants. These results demonstrate that *ATG5* mutation partially suppressed autophagic activity in RabG3bCA plants and that RabG3b-associated autophagy was at least partially ATG5 dependent. In addition, autophagic induction by RabG3bCA overexpression in the *atg5-1* mutant suggests that RabG3b may have the autophagy-independent cell death-promoting activity. Alternatively, there may be an ATG5-independent noncanonical autophagy pathway.

DISCUSSION

In this study, overexpression of a constitutively active form of *RabG3b* in plants elicited accelerated, expanded hypersensitive cell death, which was accompanied by the accumulation of abundant autophagic structures in response to the FB1 fungal toxin and avirulent bacterial pathogens. Our results suggest that Arabidopsis RabG3b regulates HR PCD during plant-pathogen interactions through its positive role in autophagy and that autophagy, as a prodeath process, contributes to hypersensitive cell death.

RabG3b Functions in Autophagy

Autophagy plays a role in the regulation of responses to various stresses, including abiotic stresses such as oxidative, salt, and drought stresses, as well as biotic stresses (Liu et al., 2005; Xiong et al., 2005, 2007; Bassham, 2007; Hofius et al., 2009; Liu and Bassham, 2012). Inoculation of RabG3bCA plants with *Pst* DC3000 (*AvrRpm1*) induced the formation of abundant autophagosome and autolysosome structures. In addition, RabG3b proteins colocalized with ATG8a proteins in autophagic structures in both *Pst* DC3000 (*AvrRpm1*)-inoculated wild-type and RabG3bCA plants. We previously demonstrated that RabG3b functions as a positive regulator of cell death during TE differentiation by activating autophagy (Kwon et al., 2010a, 2010b). Autophagic activation was remarkably increased in RabG3bCA cells during TE differentiation, leading to enhanced xylem development in both Arabidopsis and *Populus* spp. (Kwon et al., 2010a, 2011). The importance of autophagy in TE differentiation was further supported by the observation that TE formation was suppressed in *atg 5-1* mutant cells. RabG3bCA cells also accumulated numerous autophagic structures in response to Suc starvation, a general autophagy-inducing condition. Together with these findings, our results suggest that RabG3b functions as a component of plant autophagy, regulating cell death pathways associated with both plant development and stress responses.

On the other hand, RabG3bDN and RabG3bRNAi plants were not significantly different from wild-type plants with respect to both cell death and bacterial growth phenotypes. LTG-stained autophagic structures were also formed in RabG3bDN and RabG3bRNAi plants in response to *Pst* DC3000 (*AvrRpm1*) infection, although it occurred more slowly than in *Pst* DC3000 (*AvrRpm1*)-treated wild-type plants. These results suggest that the expression of dominant negative or knockdown constructs of *RabG3b* may not be sufficient for the complete abolishment of RabG3b activity. Alternatively, several autophagy pathways may redundantly operate during HR cell death. The latter possibility is supported by RabG3bCA *atg5-1* phenotypes. Whereas RabG3bCA-mediated autophagy was partially suppressed in the RabG3bCA *atg5-1* crossing line, RabG3bCA overexpression restored autophagic activity in the *atg5-1* mutant during pathogen-induced HR PCD, as determined by immunofluorescence and LTG staining. This suggests that there may be at least two autophagy pathways, ATG5 dependent and ATG5 independent, and that RabG3b may function as a common component of two pathways. The absence of a signal for autophagic activity in the pathogen-treated *atg5-1* mutant further suggests that the

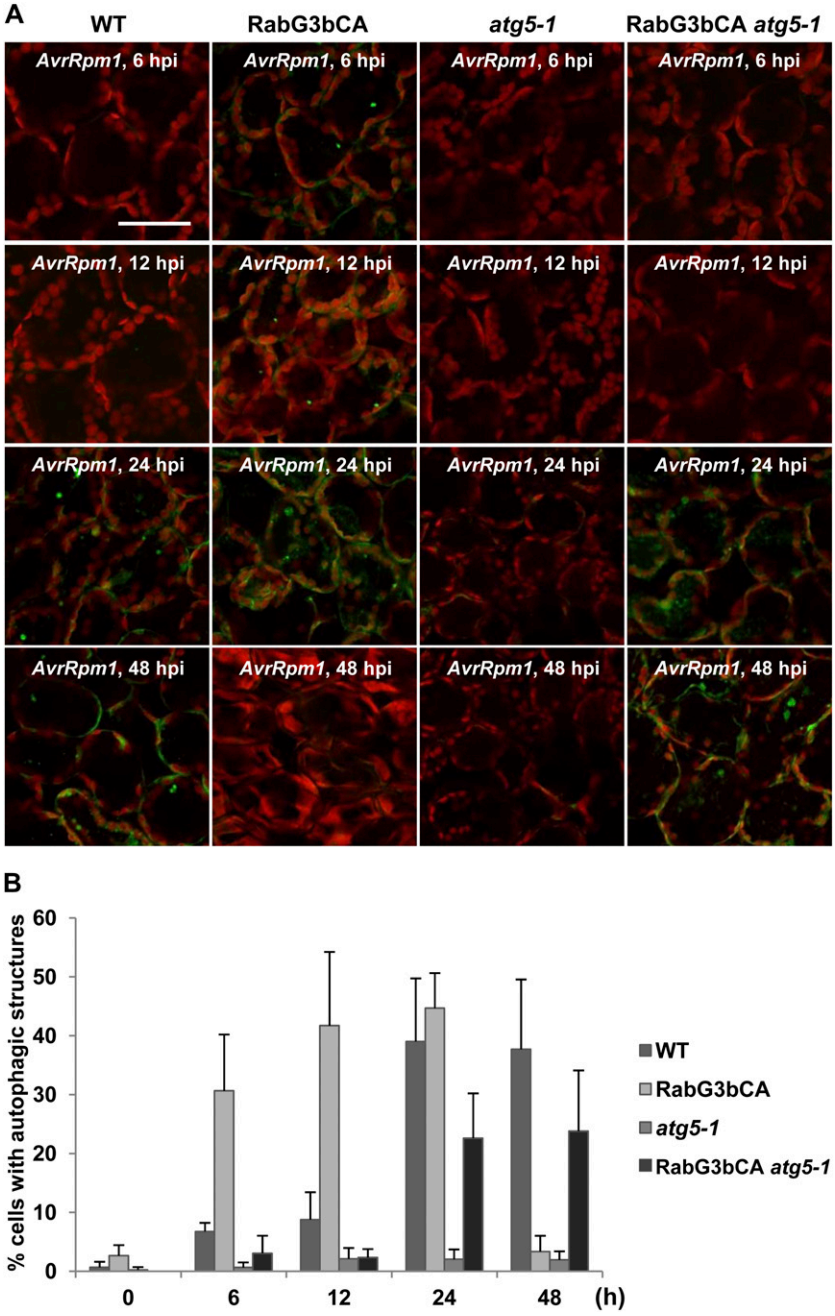

Figure 9. LTG staining of autophagic structures in RabG3bCA *atg5-1*, RabG3bCA, and *atg5-1* plants infected with *Pst* DC3000 (*AvrRpm1*). A, LTG-stained mesophyll cells at the infected sites of wild-type (WT), RabG3bCA, *atg5-1*, and RabG3bCA *atg5-1* plants treated with 10^6 cfu mL^{-1} *Pst* DC3000 (*AvrRpm1*) for 6, 12, 24, and 48 h. hpi, Hours post inoculation. Bar = 50 μm. B, Quantitative analysis of the LTG-stained structures in A. Stained tissues were photographed, and cells with fluorescent spots were counted per 250-μm^2 area. Results represent means ± SD (n = 6). These experiments were performed three times with similar results.

ATG5-dependent pathway may be dominant during immunity-triggered HR PCD. Indeed, a recent study in mouse demonstrated that mammalian macroautophagy can occur through two different pathways, an ATG5/ATG7-dependent conventional pathway and an ATG5/ATG7-independent alternative pathway (Nishida et al., 2009). It has been proposed that a noncanonical alternative autophagy pathway may also exist in plants (Li and Vierstra, 2012). However, we cannot rule out the possibility that RabG3b may be involved in an autophagy-independent cell death process.

Genetic and molecular analyses of autophagy have identified approximately 35 *ATG* genes in yeast (*Saccharomyces cerevisiae*) and many orthologs in other eukaryotes, including Arabidopsis, maize (*Zea mays*), and rice (*Oryza sativa*; Chung et al., 2009; Xia et al., 2011). ATG proteins are key players in the autophagic pathway that comprises several consecutive stages, such as target-of-rapamycin-mediated induction, vesicle nucleation and elongation of an isolation membrane or phagophore, docking and fusion of autophagosomes with lysosomes, and vesicle breakdown and degradation. Rab7 in mammals and Ypt7 in yeast have been implicated in autophagosome maturation. In mammalian cells, Rab7 colocalized with an autophagic marker, microtubule-associated protein light chain3, and was

required for the normal progression of autophagy (Gutierrez et al., 2004; Jäger et al., 2004). Fusion of autophagosomes with the vacuole was inhibited in *Ypt7* null mutants in *Saccharomyces cerevisiae* (Kirisako et al., 1999). Docking and fusion of autophagosomes was found to require the receptor complex consisting of v-SNARE VTI1, VAM3 syntaxin, and YPT7 in yeast (Thompson and Vierstra, 2005). An Arabidopsis mutant with a mutation in *VTI12*, a VTI1-type v-SNARE, exhibited a phenotype similar to that of *atg7* and *atg9* mutants characterized by accelerated chlorosis and premature leaf senescence under nutrient starvation, suggesting that VTI12 may be involved in autophagosome docking and fusion (Surpin et al., 2003). Thus, it would be valuable to examine whether RabG3b is a component of and functions in conjunction with other proteins in the SNARE complex in plants. Like Rab7 and Ypt7, RabG3b may function in autophagosome/autolysosome maturation, the late stage of autophagy. In recent studies, other Rab proteins, including Rab5, Rab32, and Rab33b, were found to be involved in autophagosome formation in mammalian autophagy (Itoh et al., 2008; Ravikumar et al., 2008; Hirota and Tanaka, 2009; Yamaguchi et al., 2009), additionally implicating RabG3b in the early stage of autophagy.

Autophagy Controls HR PCD

Despite many reports on the functions of autophagy in pathogen-induced cell death, the prosurvival or prodeath role of autophagy in plants has been controversial. Virus-induced gene silencing in tobacco led to the finding that autophagy has a prosurvival function in the pathogen-induced cell death response (Liu et al., 2005). HR PCD induced by viral infections was unrestricted and spread into uninfected cells in *BECLIN1/ATG6/VPS30-*, *PI3K/VPS34-*, *ATG3-*, and *ATG7*-silenced tobacco plants. Similar results were observed in Arabidopsis *ATG6* RNA interference and *atg5-1* mutant plants (Patel and Dinesh-Kumar, 2008; Yoshimoto et al., 2009). On the other hand, Hofius et al. (2009) reported that pathogen-induced cell death was suppressed in *atg* mutants, supporting autophagy as a prodeath process. Upon infection with the avirulent bacterial pathogens *Pst* DC3000 (*AvrRps4*) and *Pst* DC3000 (*AvrRpm1*) that depend on TIR-type immune receptors, *atg* mutants displayed reduced HR cell death, as determined by ion leakage assays and trypan blue staining of dead cells (Hofius et al., 2009). However, HR cell death in *atg* mutants was little affected by *Pst* DC3000 (*AvrRpt2*) requiring the CC-type immune receptor for activation. In contrast to *Pst* DC3000 (*AvrRpm1*), *Pst* DC3000 (*AvrRpt2*) infection induced only weak accumulation of LTG-stained structures in wild-type plants, suggesting that *AvrRpt2*-triggered HR PCD may be independent of autophagy and may require other cell death processes (Hofius et al., 2009). In our study, RabG3bCA overexpression enhanced autophagic activity and led to accelerated, expanded cell death, regardless of types of challenged avirulent pathogens, including *Pst* DC3000 (*AvrRpt2*), further supporting a prodeath role for autophagy during HR cell death. Whether autophagy contributes to hypersensitive cell death may be determined by the level of autophagic activation, which differs among distinct avirulent bacterial pathogens that activate either TIR- or CC-type immune receptors.

The prosurvival and prodeath functions of autophagy and the mechanistic interaction of autophagy with apoptosis have been important issues in our understanding of cell death pathways in animal systems (Kourtis and Tavernarakis, 2009; Scarlatti et al., 2009). Studies indicate that apoptosis and autophagy are regulated by mutual inhibition, and depending on the circumstances and the threshold, cells activate autophagy for cell survival or apoptosis for cell death (Maiuri et al., 2007). Apoptosis and autophagy are linked and coordinately regulated, sharing components in pathways (Maiuri et al., 2007; Levine et al., 2008). There are many in vivo data in animals supporting that apoptosis (type I PCD) develops due to an inhibition of autophagy. Inactivation of *ATG* genes induced apoptotic death in neurons and during *Caenorhabditis elegans* development (Takacs-Vellai et al., 2005; Hara et al., 2006; Komatsu et al., 2006). It has also been shown that cells can undergo autophagic cell death (type II PCD) depending on the stage of autophagic inhibition or the level of

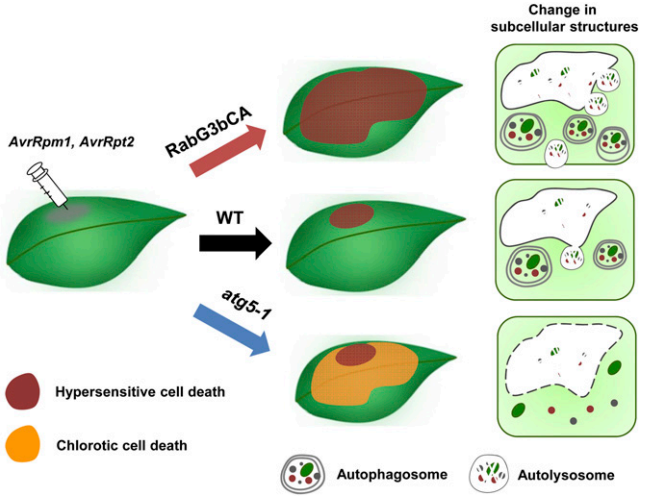

Figure 10. A model for the roles of RabG3b and autophagy in the regulation of pathogen-induced HR cell death. We propose a positive role for RabG3b in autophagy and hypersensitive cell death and both positive and negative roles for autophagy during immunity-associated HR PCD. In our model, avirulent pathogen infection readily induces HR cell death at the infected site in wild-type (WT) plants, and this is largely expanded in RabG3bCA plants but suppressed in the *atg5-1* mutant. This suggests that autophagy is a prodeath process and that autophagic cell death contributes to pathogen-induced HR PCD. On the other hand, the *atg5-1* mutant gradually develops chlorotic cell death at uninfected sites during the course of days or weeks following infection, suggesting a prosurvival role for autophagy in cellular homeostasis maintenance.

autophagic activation. When a later stage of autophagy (e.g. fusion of autophagosomes with lysosomes) is blocked or autophagy is hyperactivated, cells accumulate autophagosomes and undergo type II cell death (González-Polo et al., 2005). Autophagic cell death has been demonstrated in mammalian cells and in *Drosophila melanogaster*, *Dictyostelium discoideum*, and *C. elegans* (Shimizu et al., 2004; Yu et al., 2004; Berry and Baehrecke, 2007; Kang et al., 2007; Lam et al., 2008; Samara et al., 2008).

It has long been known that HR PCD contributes to disease resistance by physically isolating pathogens. Whereas autophagy positively affects HR cell death, it is not clear whether autophagy is involved in restricting pathogen growth at the infection site. We observed that bacterial growth in the *atg5-1* mutant was not significantly different from that in wild-type plants upon infection with *Pst* DC3000 (*AvrRpm1*) and *Pst* DC3000 (*AvrRpt2*), suggesting that autophagy may not be directly involved in limiting pathogen growth. This also implies that cell death itself may not be essential for the containment of pathogens. Many reports indicate that disease resistance is not associated with HR PCD in *dnd1/cngc2, hrl1, ndr1,* and *dnd2/hlm1/cngc4* mutant plants (Clough et al., 2000; Devadas and Raina, 2002; Balagué et al., 2003; Jurkowski et al., 2004). In *NDR1* mutant plants, resistance to avirulent *Pst* DC3000 carrying *avr* genes was compromised, but hypersensitive cell death was strain specific, such that *Pst* DC3000 (*avrRpt2*) did not develop HR but *Pst* DC3000 (*avrB*) elicited an exaggerated cell death response (Century et al., 1995; Shapiro and Zhang, 2001). Studies of the autophagic pathway in these mutants would facilitate a better understanding of the relationship between PCD, autophagy, and pathogen resistance.

In wild-type plants, *Pst* DC3000 (*AvrRpm1*) treatment readily induced autophagy at the infected site, followed by autophagic activation at uninfected sites. In fact, autophagy may play a positive role at the infected site and a negative role in uninfected tissue to regulate HR cell death during plant immunity. On the basis of both macroscopic and microscopic cell death phenotypes of pathogen-infected wild-type, RabG3bCA, and *atg5-1* mutant plants, we concluded that plants undergo two distinct cell death processes: hypersensitive cell death and chlorotic cell death (Fig. 10). The former was induced at the localized infection site of all tested plants within hours after infection and was suppressed in the *atg5-1* mutant but markedly expanded in RabG3bCA plants. This finding suggests that autophagy plays a prodeath role and that autophagic cell death contributes to cell death programs operating during pathogen-induced HR PCD. As suggested for the roles of RabG3b and autophagy during TE PCD in our previous work (Kwon et al., 2010a), autophagy-mediated degradation of cell contents and organelles may promote cytoplasm clearance after vacuole collapse during HR PCD. The latter (chlorotic cell death) occurred as a result of defective autophagy and spread beyond the infection site into uninfected sites in the *atg5-1* mutant over a period of days or weeks following infection, supporting a prosurvival role of autophagy. Pathogen-induced cell death may lead to the production of toxic materials, including reactive oxygen species, causing damage to organelles and cellular components. A prosurvival function of autophagy would be to maintain cellular homeostasis in uninfected, healthy tissues by eliminating this cellular "garbage" (Hofius et al., 2011). The increased accumulation of damaged materials in older leaves explains why chlorotic cell death is more prominent in the older *atg5-1* mutant than in younger plants, as observed in this study and previously (Yoshimoto et al., 2009). We propose that plants use prodeath and prosurvival activities of autophagy to expedite HR cell death and simultaneously limit it to the infected cells, respectively. Our proposal is substantially consistent with the view of Hofius et al. (2011) that the contradictory roles of autophagy in HR cell death proposed by different groups are the result of differences in the experimental systems (Liu et al., 2005; Patel and Dinesh-Kumar, 2008; Hofius et al., 2009; Yoshimoto et al., 2009). Additional studies on RabG3b function in membrane trafficking and autophagic processes and the identification of its interacting partners will allow a better understanding of the molecular mechanisms of autophagy during immunity-associated HR PCD.

MATERIALS AND METHODS

Plant Materials, Growth Conditions, and Treatments

Arabidopsis (*Arabidopsis thaliana*) plants (ecotype Columbia) were grown in a growth room at 24°C under long-day conditions (16-h-light/8-h-dark cycle) or in a growth chamber under short-day conditions (8-h-light/16-h-dark cycle). *Pseudomonas syringae* pv *tomato* DC3000 (*Pst* DC3000), *Pst* DC3000 (A*vrRpm1*), and *Pst* DC3000 (A*vrRpt2*) were grown on nutrient yeast extract glycerol agar medium containing 50 μg mL^{-1} rifampicin and 50 μg mL^{-1} kanamycin. To observe disease phenotypes after treatment with bacterial pathogens, leaves of 7-week-old plants grown under short-day conditions were infiltrated with 10 μL of $MgCl_2$ (10 mM) or bacterial suspensions at 10^6 to 10^8 colony-forming units (cfu) mL^{-1}. For bacterial growth assays, leaves of 7-week-old plants grown under short-day conditions were infiltrated with 10 μL of $MgCl_2$ (10 mM) or bacterial suspensions at 10^5 cfu mL^{-1}. Leaf discs (0.5 cm^2) were ground in 10 mM $MgCl_2$, serially diluted, and plated out to determine titers. For FB1 (Sigma-Aldrich) treatment, leaves of 7-week-old plants grown under short-day conditions were infiltrated with 10 μM FB1 using a 1-mL needleless syringe and kept in a growth chamber for 2 d. For flg22 treatment (Watanabe and Lam, 2006), leaves of 7-week-old plants grown under short-day conditions were infiltrated with 1 μM flg22 using a 1-mL needleless syringe and incubated in a growth chamber for the indicated times.

To generate crossing lines, RabG3bCA plants were crossed with the *atg5-1* mutant. F1 plants were selfed, and F2 seeds were harvested. The segregation of F2 seeds was confirmed by selection on kanamycin, and F2 plants were genotyped to select crossing lines. Homozygous RabG3bCA *atg5-1* crossing lines were confirmed by PCR, as described previously (Kwon et al., 2009; Yoshimoto et al., 2009).

Reverse Transcription-PCR Analysis

Total RNAs were extracted from Arabidopsis leaves using the Plant RNA Purification Reagent (Invitrogen). First-strand complementary DNAs were synthesized from 1 μg of total RNAs using the Power cDNA Synthesis Kit (iNtRON). PCR reactions were performed with the following gene-specific primers: for *PR1*,

5′-ATGAATTTTACTGGCTATTC-3′ and 5′-TTAGTATGGCTTCTCGTTC-3′; for *FRK1*, 5′-GCTGGATCCATCGGTTACCTTGAC-3′ and 5′-TAGATTCACTGTAAGCATTTTCGT-3′; and for *Actin*, 5′-GGCGATGAAGCTCAATCCAAACG-3′ and 5′-GGTCACGACCAGCAAGATCAAGACG-3′.

Trypan Blue Staining

Trypan blue staining was performed as described previously (Bowling et al., 1997). Samples were submerged in lactic acid-phenol-trypan blue solution (2.5 mg mL^{-1} trypan blue, 25% lactic acid, 23% water-saturated phenol, and 25% glycerol) and boiled for 1 min. Stained samples were then placed in a 60% chloral hydrate solution and finally equilibrated with 50% glycerol.

Ion Leakage Assay

Ion leakage experiments were performed as described previously (Mackey et al., 2003). Leaves of 5-week-old plants grown under long-day conditions were infiltrated with bacterial suspensions of *Pst* DC3000 (*AvrRpm1*) at 2×10^8 cfu mL^{-1}. Ten leaf discs (0.5 cm^2) were immediately removed and floated in 30 mL of distilled water for washing. After 30 min, washed leaf discs were moved into 10 mL of fresh distilled water. Ion conductance was then measured over time using a conductivity meter (Thermo Scientific).

Callose Deposition Assay

Callose deposition was visualized by aniline blue staining as described previously (Jacobs et al., 2003; Clay et al., 2009). Arabidopsis leaves were harvested 1 d after treatment with 1 μM flg22 and fixed in acetic acid:ethanol (1:3) for 8 h with two solution changes. Leaves were then incubated in 50% ethanol for 1 h, 30% ethanol for 1 h, and finally distilled water for 2 h with two solution changes. Leaves were then stained with 5 mg mL^{-1} aniline blue in 150 mM sodium phosphate (pH 7.0) in the dark for 1 h and mounted on slides using 50% glycerol. Callose was observed under a confocal microscope (Zeiss LSM 510 META).

LTG Staining

LTG staining was performed as described previously (Liu et al., 2005; Patel and Dinesh-Kumar, 2008). Leaf pieces were infiltrated with 1 μM LTG DND-26 (Molecular Probes) and incubated in the dark for 1 h. Images were acquired using a confocal microscope (Zeiss LSM 510 META). The wavelengths used for LTG and chloroplasts were 488 to 505 nm and 565 to 625 nm, respectively.

Antibody Preparation

The full-length coding region of *ATG8a* was cloned into the pET15b vector (Novagen) and used for the transformation of *Escherichia coli* (BL21) cells. Production of recombinant ATG8a proteins was induced by the addition of 1 mM isopropylthio-β-galactoside for 2 h, and the proteins were purified using a nickel-nitrilotriacetic acid agarose column according to the manufacturer's instructions (Qiagen). Affinity-purified recombinant proteins were used to raise the anti-ATG8a antibody in rats. The anti-RabG3b antibody was raised in rabbits as described previously (Kwon et al., 2009).

Immunoblot Analysis

Western-blot analysis was performed as described previously (Yoshimoto et al., 2004; Chung et al., 2009). Seven-week-old plants grown under short-day conditions were used, and protein samples were prepared from leaves treated with *Pst* DC3000 (*AvrRpm1*) at 10^6 cfu mL^{-1}. Total proteins were separated by 12% SDS-PAGE in the presence of 6 M urea and electrophoretically transferred onto nitrocellulose membranes. The blots were probed with the ATG8a antibody overnight at 4°C. Following incubation with secondary antibody conjugated to horseradish peroxidase, antibody-bound proteins were detected using the enhanced chemiluminescence system (GE Healthcare).

Whole-Mount Immunofluorescence Analysis

Whole-mount immunofluorescence experiments were performed as described previously (Leivar et al., 2005). Leaf discs (0.5 cm^2) were fixed in 4% formaldehyde dissolved in PMEG buffer (50 mM PIPES, pH 6.9, 5 mM $MgSO_4$, and 5 mM EGTA) and 10% dimethyl sulfoxide for 3 h at room temperature under vacuum. Samples were washed three times with PMEG buffer and incubated in PMEG buffer containing 0.5% pectolyase (Sigma), 0.5% Triton X-100, and 1% bovine serum albumin (BSA) for 30 min at 37°C. Samples were then washed six times with PMEG buffer and incubated with the anti-ATG8a antibody in 0.1 M phosphate-buffered saline (PBS) containing 3% BSA overnight at 4°C. After washing with PBS, samples were incubated with fluorescein isothiocyanate-conjugated goat anti-rat IgG (AlexaFluor 488; Invitrogen) for 3 h at room temperature and washed three additional times with PBS. Samples were observed with a confocal microscope (Zeiss LSM 510 META) at 488/505-nm excitation/emission.

Electron Microscopy Analysis

Leaves were fixed in a solution containing 2.5% glutaraldehyde and 4% paraformaldehyde in 0.1 M phosphate buffer (pH 7.4) for 4 h at 4°C, rinsed in 0.1 M phosphate buffer (pH 7.4), and further fixed in 1% OsO_4 for 4 h at 4°C. After rinsing, samples were dehydrated and embedded in LR White resin (London Resin). For TEM analysis, thin sections (40–50 nm thickness) collected on nickel grids (1-GN; 150 mesh) were stained with uranyl acetate and lead citrate and examined by TEM (Tecnai 12; Philips). For immunogold electron microscopy analysis, sections collected on copper grids were blocked with BSA-TBST buffer (500 mM NaCl, 1% BSA, 0.3% Tween 20, and 10 mM Tris-HCl, pH 7.4) for 1 h and incubated with an anti-RabG3b antibody (rabbit) and/or an anti-ATG8a antibody (rat) for 4 h at room temperature. Samples were rinsed in BSA-TBST buffer, and primary antibody binding was detected using anti-rabbit IgG (5-nm gold; Electron Microscopy Sciences) and anti-rat IgG (1-nm gold; Sigma). After washing with TBST and distilled water, samples were stained with uranyl acetate and observed by TEM.

Sequence data from this article can be found in the GenBank/EMBL data libraries under accession number At1g22740 (RabG3b).

Supplemental Data

The following materials are available in the online version of this article.

Supplemental Figure S1. Cell-death phenotypes of leaves inoculated with *Pst* DC3000 (*AvrRpm1*) in 5-week-old young plants.

Supplemental Figure S2. Cell-death phenotypes of leaves inoculated with *Pst* DC3000 (*AvrRpt2*) and FB1.

Supplemental Figure S3. Bacterial growth in wild-type, RabG3bCA, RabG3bDN, RabG3bRNAi, and *atg5-1* plants.

Supplemental Figure S4. Basal immunity is not defective in RabG3bCA and *atg5-1* plants.

Supplemental Figure S5. Autophagy is induced at both the infected and uninfected sites of plants following *Pst* DC3000 (*AvrRpm1*) infection.

Supplemental Figure S6. Autophagic structures are formed in wild-type plants and more abundantly in RabG3bCA plants following *Pst* DC3000 (*AvrRpt2*) infection.

Supplemental Figure S7. TEM images of autophagic structures in wild-type, RabG3bCA, and *atg5-1* plants inoculated with *Pst* DC3000 (*AvrRpm1*).

Supplemental Figure S8. Bacterial growth in wild-type, RabG3bCA, *atg5-1*, and RabG3bCA *atg5-1* plants.

Supplemental Figure S9. Whole-mount immunofluorescence staining of *Pst* DC3000 (*AvrRpm1*)-infected wild-type, RabG3bCA, RabG3bCA *atg5-1*, and *atg5-1* plants with the anti-ATG8a antibody.

ACKNOWLEDGMENTS

We thank Dr. Richard D. Vierstra for *atg5-1* seeds.

Received September 25, 2012; accepted February 8, 2013; published February 12, 2013.

LITERATURE CITED

Balagué C, Lin B, Alcon C, Flottes G, Malmström S, Köhler C, Neuhaus G, Pelletier G, Gaymard F, Roby D (2003) HLM1, an essential signaling component in the hypersensitive response, is a member of the cyclic nucleotide-gated channel ion channel family. Plant Cell **15:** 365–379

Bassham DC (2007) Plant autophagy: more than a starvation response. Curr Opin Plant Biol **10:** 587–593

Berry DL, Baehrecke EH (2007) Growth arrest and autophagy are required for salivary gland cell degradation in Drosophila. Cell **131:** 1137–1148

Boller T, He SY (2009) Innate immunity in plants: an arms race between pattern recognition receptors in plants and effectors in microbial pathogens. Science **324:** 742–744

Bowling SA, Clarke JD, Liu Y, Klessig DF, Dong X (1997) The *cpr5* mutant of *Arabidopsis* expresses both NPR1-dependent and NPR1-independent resistance. Plant Cell **9:** 1573–1584

Century KS, Holub EB, Staskawicz BJ (1995) NDR1, a locus of Arabidopsis thaliana that is required for disease resistance to both a bacterial and a fungal pathogen. Proc Natl Acad Sci USA **92:** 6597–6601

Chung T (2011) See how I eat my green: autophagy in plant cells. J Plant Biol **54:** 339–350

Chung T, Suttangkakul A, Vierstra RD (2009) The ATG autophagic conjugation system in maize: ATG transcripts and abundance of the ATG8-lipid adduct are regulated by development and nutrient availability. Plant Physiol **149:** 220–234

Clay NK, Adio AM, Denoux C, Jander G, Ausubel FM (2009) Glucosinolate metabolites required for an Arabidopsis innate immune response. Science **323:** 95–101

Clough SJ, Fengler KA, Yu IC, Lippok B, Smith RK Jr, Bent AF (2000) The Arabidopsis dnd1 "defense, no death" gene encodes a mutated cyclic nucleotide-gated ion channel. Proc Natl Acad Sci USA **97:** 9323–9328

Coll NS, Epple P, Dangl JL (2011) Programmed cell death in the plant immune system. Cell Death Differ **18:** 1247–1256

Devadas SK, Raina R (2002) Preexisting systemic acquired resistance suppresses hypersensitive response-associated cell death in Arabidopsis *hrl1* mutant. Plant Physiol **128:** 1234–1244

Dodds PN, Rathjen JP (2010) Plant immunity: towards an integrated view of plant-pathogen interactions. Nat Rev Genet **11:** 539–548

González-Polo RA, Boya P, Pauleau AL, Jalil A, Larochette N, Souquère S, Eskelinen EL, Pierron G, Saftig P, Kroemer G (2005) The apoptosis/autophagy paradox: autophagic vacuolization before apoptotic death. J Cell Sci **118:** 3091–3102

Gunawardena AH (2008) Programmed cell death and tissue remodelling in plants. J Exp Bot **59:** 445–451

Gutierrez MG, Munafó DB, Berón W, Colombo MI (2004) Rab7 is required for the normal progression of the autophagic pathway in mammalian cells. J Cell Sci **117:** 2687–2697

Hara T, Nakamura K, Matsui M, Yamamoto A, Nakahara Y, Suzuki-Migishima R, Yokoyama M, Mishima K, Saito I, Okano H, et al (2006) Suppression of basal autophagy in neural cells causes neurodegenerative disease in mice. Nature **441:** 885–889

Hara-Nishimura I, Hatsugai N, Nakaune S, Kuroyanagi M, Nishimura M (2005) Vacuolar processing enzyme: an executor of plant cell death. Curr Opin Plant Biol **8:** 404–408

Hatsugai N, Iwasaki S, Tamura K, Kondo M, Fuji K, Ogasawara K, Nishimura M, Hara-Nishimura I (2009) A novel membrane fusion-mediated plant immunity against bacterial pathogens. Genes Dev **23:** 2496–2506

Hayward AP, Dinesh-Kumar SP (2011) What can plant autophagy do for an innate immune response? Annu Rev Phytopathol **49:** 557–576

Hirota Y, Tanaka Y (2009) A small GTPase, human Rab32, is required for the formation of autophagic vacuoles under basal conditions. Cell Mol Life Sci **66:** 2913–2932

Hofius D, Munch D, Bressendorff S, Mundy J, Petersen M (2011) Role of autophagy in disease resistance and hypersensitive response-associated cell death. Cell Death Differ **18:** 1257–1262

Hofius D, Schultz-Larsen T, Joensen J, Tsitsigiannis DI, Petersen NH, Mattsson O, Jørgensen LB, Jones JD, Mundy J, Petersen M (2009) Autophagic components contribute to hypersensitive cell death in Arabidopsis. Cell **137:** 773–783

Itoh T, Fujita N, Kanno E, Yamamoto A, Yoshimori T, Fukuda M (2008) Golgi-resident small GTPase Rab33B interacts with Atg16L and modulates autophagosome formation. Mol Biol Cell **19:** 2916–2925

Jacobs AK, Lipka V, Burton RA, Panstruga R, Strizhov N, Schulze-Lefert P, Fincher GB (2003) An *Arabidopsis* callose synthase, GSL5, is required for wound and papillary callose formation. Plant Cell **15:** 2503–2513

Jäger S, Bucci C, Tanida I, Ueno T, Kominami E, Saftig P, Eskelinen EL (2004) Role for Rab7 in maturation of late autophagic vacuoles. J Cell Sci **117:** 4837–4848

Jones JD, Dangl JL (2006) The plant immune system. Nature **444:** 323–329

Joubert PE, Meiffren G, Grégoire IP, Pontini G, Richetta C, Flacher M, Azocar O, Vidalain PO, Vidal M, Lotteau V, et al (2009) Autophagy induction by the pathogen receptor CD46. Cell Host Microbe **6:** 354–366

Jurkowski GI, Smith RK Jr, Yu IC, Ham JH, Sharma SB, Klessig DF, Fengler KA, Bent AF (2004) Arabidopsis DND2, a second cyclic nucleotide-gated ion channel gene for which mutation causes the "defense, no death" phenotype. Mol Plant Microbe Interact **17:** 511–520

Kang C, You YJ, Avery L (2007) Dual roles of autophagy in the survival of *Caenorhabditis elegans* during starvation. Genes Dev **21:** 2161–2171

Kirisako T, Baba M, Ishihara N, Miyazawa K, Ohsumi M, Yoshimori T, Noda T, Ohsumi Y (1999) Formation process of autophagosome is traced with Apg8/Aut7p in yeast. J Cell Biol **147:** 435–446

Komatsu M, Waguri S, Chiba T, Murata S, Iwata J, Tanida I, Ueno T, Koike M, Uchiyama Y, Kominami E, et al (2006) Loss of autophagy in the central nervous system causes neurodegeneration in mice. Nature **441:** 880–884

Kourtis N, Tavernarakis N (2009) Autophagy and cell death in model organisms. Cell Death Differ **16:** 21–30

Kuriyama H, Fukuda H (2002) Developmental programmed cell death in plants. Curr Opin Plant Biol **5:** 568–573

Kwon SI, Cho HJ, Bae K, Jung JH, Jin HC, Park OK (2009) Role of an Arabidopsis Rab GTPase RabG3b in pathogen response and leaf senescence. J Plant Biol **52:** 79–87

Kwon SI, Cho HJ, Jung JH, Yoshimoto K, Shirasu K, Park OK (2010a) The Rab GTPase RabG3b functions in autophagy and contributes to tracheary element differentiation in Arabidopsis. Plant J **64:** 151–164

Kwon SI, Cho HJ, Lee JS, Jin H, Shin SJ, Kwon M, Noh EW, Park OK (2011) Overexpression of constitutively active Arabidopsis RabG3b promotes xylem development in transgenic poplars. Plant Cell Environ **34:** 2212–2224

Kwon SI, Cho HJ, Park OK (2010b) Role of Arabidopsis RabG3b and autophagy in tracheary element differentiation. Autophagy **6:** 1187–1189

Lai Z, Wang F, Zheng Z, Fan B, Chen Z (2011) A critical role of autophagy in plant resistance to necrotrophic fungal pathogens. Plant J **66:** 953–968

Lam D, Kosta A, Luciani MF, Golstein P (2008) The inositol 1,4,5-trisphosphate receptor is required to signal autophagic cell death. Mol Biol Cell **19:** 691–700

Leivar P, González VM, Castel S, Trelease RN, López-Iglesias C, Arró M, Boronat A, Campos N, Ferrer A, Fernàndez-Busquets X (2005) Subcellular localization of Arabidopsis 3-hydroxy-3-methylglutaryl-coenzyme A reductase. Plant Physiol **137:** 57–69

Lenz HD, Haller E, Melzer E, Kober K, Wurster K, Stahl M, Bassham DC, Vierstra RD, Parker JE, Bautor J, et al (2011) Autophagy differentially controls plant basal immunity to biotrophic and necrotrophic pathogens. Plant J **66:** 818–830

Levine B (2005) Eating oneself and uninvited guests: autophagy-related pathways in cellular defense. Cell **120:** 159–162

Levine B, Mizushima N, Virgin HW (2011) Autophagy in immunity and inflammation. Nature **469:** 323–335

Levine B, Sinha S, Kroemer G (2008) Bcl-2 family members: dual regulators of apoptosis and autophagy. Autophagy **4:** 600–606

Li F, Vierstra RD (2012) Autophagy: a multifaceted intracellular system for bulk and selective recycling. Trends Plant Sci **17:** 526–537

Liu Y, Bassham DC (2012) Autophagy: pathways for self-eating in plant cells. Annu Rev Plant Biol **63:** 215–237

Liu Y, Schiff M, Czymmek K, Tallóczy Z, Levine B, Dinesh-Kumar SP (2005) Autophagy regulates programmed cell death during the plant innate immune response. Cell **121:** 567–577

Mackey D, Belkhadir Y, Alonso JM, Ecker JR, Dangl JL (2003) Arabidopsis RIN4 is a target of the type III virulence effector AvrRpt2 and modulates RPS2-mediated resistance. Cell **112:** 379–389

Maiuri MC, Zalckvar E, Kimchi A, Kroemer G (2007) Self-eating and self-killing: crosstalk between autophagy and apoptosis. Nat Rev Mol Cell Biol **8:** 741–752

Naito K, Taguchi F, Suzuki T, Inagaki Y, Toyoda K, Shiraishi T, Ichinose Y (2008) Amino acid sequence of bacterial microbe-associated molecular

pattern flg22 is required for virulence. Mol Plant Microbe Interact **21:** 1165–1174

Nishida Y, Arakawa S, Fujitani K, Yamaguchi H, Mizuta T, Kanaseki T, Komatsu M, Otsu K, Tsujimoto Y, Shimizu S (2009) Discovery of Atg5/Atg7-independent alternative macroautophagy. Nature **461:** 654–658

Oh IS, Park AR, Bae MS, Kwon SJ, Kim YS, Lee JE, Kang NY, Lee S, Cheong H, Park OK (2005) Secretome analysis reveals an *Arabidopsis* lipase involved in defense against *Alternaria brassicicola*. Plant Cell **17:** 2832–2847

Patel S, Dinesh-Kumar SP (2008) Arabidopsis ATG6 is required to limit the pathogen-associated cell death response. Autophagy **4:** 20–27

Ravikumar B, Imarisio S, Sarkar S, O'Kane CJ, Rubinsztein DC (2008) Rab5 modulates aggregation and toxicity of mutant huntingtin through macroautophagy in cell and fly models of Huntington disease. J Cell Sci **121:** 1649–1660

Samara C, Syntichaki P, Tavernarakis N (2008) Autophagy is required for necrotic cell death in *Caenorhabditis elegans*. Cell Death Differ **15:** 105–112

Scarlatti F, Granata R, Meijer AJ, Codogno P (2009) Does autophagy have a license to kill mammalian cells? Cell Death Differ **16:** 12–20

Schmid D, Münz C (2007) Innate and adaptive immunity through autophagy. Immunity **27:** 11–21

Shapiro AD, Zhang C (2001) The role of NDR1 in avirulence gene-directed signaling and control of programmed cell death in Arabidopsis. Plant Physiol **127:** 1089–1101

Shimizu S, Kanaseki T, Mizushima N, Mizuta T, Arakawa-Kobayashi S, Thompson CB, Tsujimoto Y (2004) Role of Bcl-2 family proteins in a non-apoptotic programmed cell death dependent on autophagy genes. Nat Cell Biol **6:** 1221–1228

Surpin M, Zheng H, Morita MT, Saito C, Avila E, Blakeslee JJ, Bandyopadhyay A, Kovaleva V, Carter D, Murphy A, et al (2003) The VTI family of SNARE proteins is necessary for plant viability and mediates different protein transport pathways. Plant Cell **15:** 2885–2899

Takacs-Vellai K, Vellai T, Puoti A, Passannante M, Wicky C, Streit A, Kovacs AL, Müller F (2005) Inactivation of the autophagy gene bec-1 triggers apoptotic cell death in C. elegans. Curr Biol **15:** 1513–1517

Thompson AR, Vierstra RD (2005) Autophagic recycling: lessons from yeast help define the process in plants. Curr Opin Plant Biol **8:** 165–173

Tsuda K, Katagiri F (2010) Comparing signaling mechanisms engaged in pattern-triggered and effector-triggered immunity. Curr Opin Plant Biol **13:** 459–465

van Doorn WG, Beers EP, Dangl JL, Franklin-Tong VE, Gallois P, Hara-Nishimura I, Jones AM, Kawai-Yamada M, Lam E, Mundy J, et al (2011) Morphological classification of plant cell deaths. Cell Death Differ **18:** 1241–1246

Via LE, Fratti RA, McFalone M, Pagan-Ramos E, Deretic D, Deretic V (1998) Effects of cytokines on mycobacterial phagosome maturation. J Cell Sci **111:** 897–905

Watanabe N, Lam E (2006) Arabidopsis Bax inhibitor-1 functions as an attenuator of biotic and abiotic types of cell death. Plant J **45:** 884–894

Xia K, Liu T, Ouyang J, Wang R, Fan T, Zhang M (2011) Genome-wide identification, classification, and expression analysis of autophagy-associated gene homologues in rice (*Oryza sativa* L.). DNA Res **18:** 363–377

Xiong Y, Contento AL, Bassham DC (2005) AtATG18a is required for the formation of autophagosomes during nutrient stress and senescence in *Arabidopsis thaliana*. Plant J **42:** 535–546

Xiong Y, Contento AL, Nguyen PQ, Bassham DC (2007) Degradation of oxidized proteins by autophagy during oxidative stress in Arabidopsis. Plant Physiol **143:** 291–299

Yamaguchi H, Nakagawa I, Yamamoto A, Amano A, Noda T, Yoshimori T (2009) An initial step of GAS-containing autophagosome-like vacuoles formation requires Rab7. PLoS Pathog **5:** e1000670

Yoshimoto K, Hanaoka H, Sato S, Kato T, Tabata S, Noda T, Ohsumi Y (2004) Processing of ATG8s, ubiquitin-like proteins, and their deconjugation by ATG4s are essential for plant autophagy. Plant Cell **16:** 2967–2983

Yoshimoto K, Jikumaru Y, Kamiya Y, Kusano M, Consonni C, Panstruga R, Ohsumi Y, Shirasu K (2009) Autophagy negatively regulates cell death by controlling NPR1-dependent salicylic acid signaling during senescence and the innate immune response in *Arabidopsis*. Plant Cell **21:** 2914–2927

Yu L, Alva A, Su H, Dutt P, Freundt E, Welsh S, Baehrecke EH, Lenardo MJ (2004) Regulation of an ATG7-beclin 1 program of autophagic cell death by caspase-8. Science **304:** 1500–1502